# Product-induced corrosion of Pt / graphite during catalytic oxidation of sorbose studied by in situ STM and cyclic voltammetry

I. Bakos [*], T. Mallat and A. Baiker [‡]

*Department of Chemical Engineering and Industrial Chemistry, Swiss Federal Institute of Technology, ETH-Zentrum, CH-8092 Zurich, Switzerland*

Received 18 July 1996; accepted 16 November 1996

Platinum deposited onto high and low surface area graphites are used as model catalysts in studying the irreversible catalyst deactivation observed previously in the aerobic oxidation of L-sorbose to 2-keto-L-gulonic acid. The corrosion of platinum in the neutral aqueous solution was followed in the liquid cell of a scanning tunnelling microscope. Leaching of platinum was well detectable in the time scale of 1–2 h. Depending on the nature of graphite support and the Pt content, a considerable fraction or even all Pt dissolved during sorbose oxidation, as evidenced by cyclic voltammetry. The strikingly high rate of Pt dissolution into the neutral aqueous medium under ambient conditions is attributed to the excellent chelating properties of the polyhydroxy carboxylic acid product.

**Keywords:** Pt / graphite, corrosion, sorbose oxidation, scanning tunnelling microscopy, cyclic voltammetry

## 1. Introduction

Selective oxidation of alcohols to carbonyl compounds or carboxylic acids over platinum metal catalyst has received much attention from both industrial and academic sides [1–3]. Important benefits of the process are that air or oxygen can be used as oxidant in aqueous solutions under mild conditions: very attractive conditions for the transformation of polyols and carbohydrates [4–10].

Extensive effort [11-14] has been made to apply this method in the direct oxidation of L-sorbose (without protection with acetone, scheme 1) to 2-keto-L-gulonic acid, an important intermediate in vitamin C synthesis [15]. However, a remarkable deactivation of Pt- and Pd-based mono and bimetallic catalysts is observed in a neutral aqueous solution and near ambient temperature, which conditions are the best for the selective oxidation of the C-1 hydroxyl group of L-sorbose [16]. It has been shown for Bi-promoted Pt / alumina that besides catalyst poisoning (i.e. by-product formation and their strong adsorption on the active sites) there is an irreversible deactivation due to corrosive restructuring of the catalyst. X-ray photoelectron spectroscopic (XPS) analysis before and after reaction evidenced the rapid dissolution of the bismuth promoter. Simultaneously, a minor decrease of the Pt content of the catalyst was also detected by means of atomic emission spectroscopy, but XPS and transmission electron microscopic (TEM) measurements failed to confirm the Pt loss.

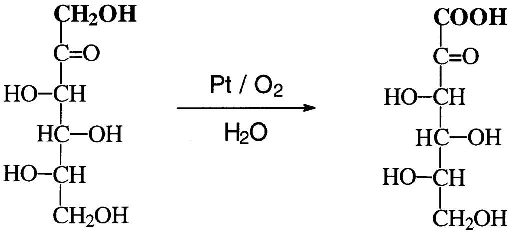

Scheme 1.

This type of irreversible deactivation has also been observed in other platinum-metal-catalyzed oxidations. A considerable loss of the Pd content of a Pd / $CaCO_3$ catalyst has been noticed after its repeated use in the oxidation of 2-methylphenoxyethanol [12], and an increase in particle size due to dissolution and redeposition of Pt onto the carbon support was observed by TEM after the oxidation of methyl-$\alpha$-D-glucoside [17].

The aim of the present study was the direct investigation of the leaching of Pt during the aqueous phase oxidation of L-sorbose by means of cyclic voltammetry and in situ scanning tunnelling microscopy (STM). Model catalysts consisting of platinum supported on various graphites, suitable for electrochemical and STM investigations [18–27], were used for this purpose.

## 2. Experimental

Solutions were prepared from analytical grade chemicals using "water for HPLC" (Fluka). All experiments were carried out at room temperature.

---

[*] Present address: Central Research Institute for Chemistry, Hungarian Academy of Sciences, H-1525 Budapest, PO Box 17, Hungary.

[‡] To whom correspondence should be addressed.

### 2.1. Preparation of Pt/graphite

Three types of graphite were used as support:

(a) graphite tablets made by pressing graphite powder (Lonza SPG 75, BET: 75 $m^2g^{-1}$) with 0.2 N $m^{-2}$;

(b) graphite paste (Metrohm, frequently used as "carbon paste electrode" material [28]);

(c) highly oriented pyrolytic graphite (HOPG, Advanced Ceramics Co., freshly cleaved before platinum deposition).

The exposed area of graphite electrodes was 0.16 $cm^2$ in all experiments.

Platinum deposition onto graphite was made electrolytically at constant potential values from solution A ($10^{-1}$ mol $\ell^{-1}$ HCl and $2 \times 10^{-2}$ mol $\ell^{-1}$ $H_2PtCl_6$) or solution B ($10^{-3}$ mol $\ell^{-1}$ $H_2SO_4$ and $10^{-3}$ mol $\ell^{-1}$ $H_2PtCl_6$). During platinum deposition the current vs. time curves were recorded. It was found that a significant overpotential is required for Pt deposition onto graphite tablets. The charge used for the deposition ($Q_d$) was calculated from these curves. The conditions of Pt deposition are summarized in table 1.

### 2.2. Electrochemical polarization (cyclic voltammetry)

Cyclic voltammograms were measured in 0.5 mol $\ell^{-1}$ $H_2SO_4$ using a conventional electrochemical cell equipped with a Pt counter electrode and a hydrogen electrode immersed in the same solution, as reference. All potentials in the text are given on the RHE (reference hydrogen electrode) scale. Bubbling $N_2$ (99.995%) was used to deoxygenate the solutions before voltammetric runs.

The amount of deposited Pt was estimated from the charge consumed during Pt deposition ($Q_d$). The apparent quantities of deposited Pt, considering only the $Pt^{4+} \rightarrow Pt^0$ reaction, indicate the possible maximum amount of Pt deposited onto graphite. Taking into account the contribution of the $Pt^{4+} \rightarrow Pt^{2+}$ reaction, i.e. the partial reduction of the precursor without metal deposition, the real quantity of deposited Pt is considerably smaller. In practice, the real amount of deposited Pt can be half of the apparent value [29], but the actual value is likely a function of the nature of the graphite support.

Table 1
Pt/graphite samples used in cyclic voltammetric and STM studies

| | Pt/graphite tablet | Pt/graphite paste | Pt/HOPG | |
|---|---|---|---|---|
| | (fig. 1) | (fig. 2) | (fig. 3) | (fig. 5) |
| Pt solution [a] | A | B | B | B |
| $E_d$ [b] (mV) | 150 | 450 | 600 | 350 |
| $Q_d$ [c] (mC) | 1200 | 1 | 0.25 | 10 |
| Pt amount [d] ($\mu$g) | 600 | 0.5 | 0.125 | 5 |
| Pt surface [e] ($cm^2$) | 35 | 0.14 | 0.06 | – |

[a] See Experimental.
[b] Potential of Pt deposition.
[c] Cathodic charge consumed during Pt deposition.
[d] Apparent quantity of Pt, calculated from the charge consumed during Pt deposition (see Experimental).
[e] Calculated from hydrogen sorption (see Experimental).

The real surface area of Pt particles was determined from the area under the hydrogen sorption peaks of the voltammograms, assuming that 210 $\mu$C charge is equivalent to 1 $cm^2$ [30]. These data are also collected in table 1.

### 2.3. Scanning tunnelling microscopy

STM measurements were performed using a commercial instrument (Topometrix, TMX 2000, equipped with an electrochemistry cell and DM1000 bipotentiostat). Tunnelling tips were formed by cutting mechanically a Pt/Ir wire (80/20%, diameter: 0.25 mm). For in situ measurements the tips were coated with paraffin wax. All images were recorded with the constant current mode; tunnelling current ranged from 0.5 to 2 nA, and sample bias from 50 to 100 mV.

### 2.4. Oxidation of L-sorbose

40 g $\ell^{-1}$ aqueous L-sorbose solution was used at room temperature and the pH was adjusted to 7.2 by $NaHCO_3$. These conditions have been found to be optimal for sorbose oxidation with Pt and air [16]. There was no mixing or forced absorption of air into the solution. Consequently, the model "reactor" worked under oxygen mass transport limitation, which has been found to be advantageous to avoid the deactivation of Pt by "over-oxidation" [5,31,32].

## 3. Results

Platinum deposited onto graphite was immersed into a neutral aqueous L-sorbose solution at ambient air. Morphological changes of Pt during L-sorbose oxidation were monitored ex situ by cyclic voltammetric runs and in situ in the liquid cell of a scanning tunnelling microscope.

### 3.1. Voltammetric studies

Figs. 1a, 2c and 3a (dashed line) depict the cyclic voltammetric curves of graphite supports. A minor double layer capacity could be observed in the case of HOPG (very low surface area) and graphite paste, whereas a considerable capacity was found with the tablets made of graphite powder (relatively high BET surface area).

During Pt deposition onto graphite supports the conditions were chosen so as to obtain relatively low Pt loading. The minimum Pt content was limited by the detectability of the current peaks for hydrogen sorption and ionization ("hydrogen region" of the voltammo-

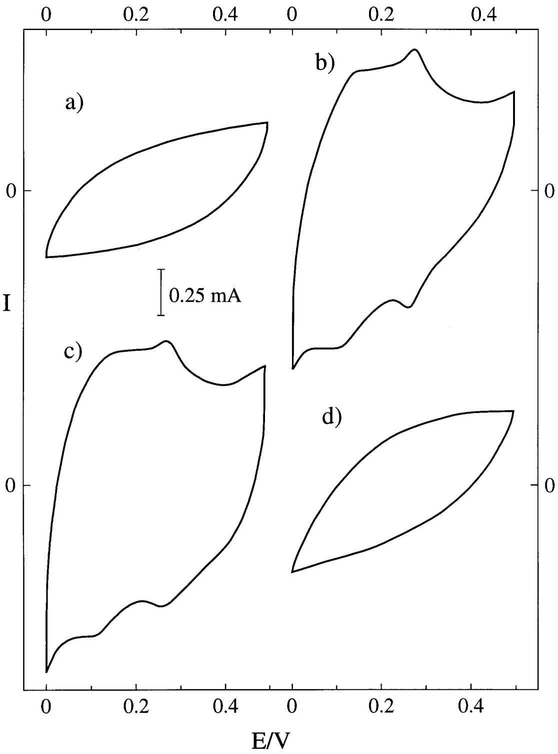

Fig. 1. Cyclic voltammetric curves of a graphite tablet before Pt deposition (a) and after Pt deposition (b). Voltammograms measured after keeping the Pt/graphite in 40 g $\ell^{-1}$ aqueous L-sorbose solution (pH = 7.2) in air for 24 and 120 h are shown by curves (c) and (d), respectively (sweep rate: 10 mV $s^{-1}$, 0.5 mol $\ell^{-1}$ $H_2SO_4$).

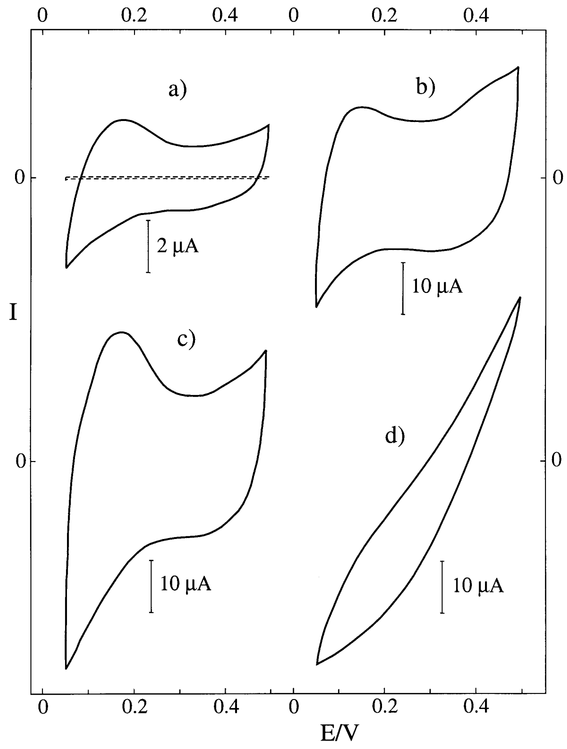

Fig. 3. Cyclic voltammograms of a HOPG (a, dashed line) and a Pt/HOPG sample (a, solid line). Voltammograms measured after keeping the Pt/HOPG in 40 g $\ell^{-1}$ aqueous sorbose solution (pH = 7.2) in air for 24, 72 and 120 h are shown by curves (b), (c) and (d), respectively (sweep rate: 10 mV $s^{-1}$, 0.5 mol $\ell^{-1}$ $H_2SO_4$).

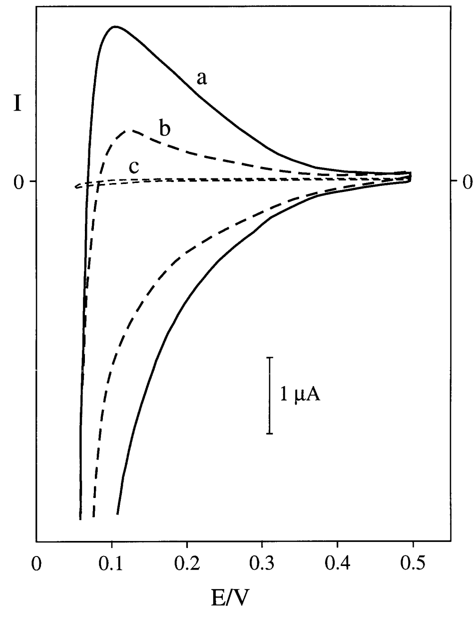

Fig. 2. Cyclic voltammograms of a Pt/graphite paste sample before (a) and after sorbose oxidation for 120 h (b), and that of the graphite paste before Pt deposition (c) (sweep rate: 10 mV $s^{-1}$, 0.5 mol $\ell^{-1}$ $H_2SO_4$).

grams below ca. 0.35 V). Voltammograms of the Pt/graphite samples are presented in figs. 1b, 2a and in fig. 3a (solid line). The characteristics of Pt/graphite samples, including the amount and surface area of Pt, are listed in table 1.

After characterisation, the Pt/graphite samples were kept in aqueous L-sorbose solution (under open circuit) exposed to air at ambient conditions. These experiments mimic the conditions of the aerobic oxidation of sorbose over supported Pt catalysts [16]. In order to gain information on the surface state of the catalysts, the cyclic voltammograms were repeatedly measured (after removing the samples from the reactor and rinsing them carefully with distilled water). Figs. 1c and 1d, 2b and 3b–3d indicate dramatic changes compared to the original voltammograms. In the case of the graphite tablet (fig. 1), the voltammogram measured after 120 h (fig. 1d) practically coincides with that of the unloaded support (fig. 1a), demonstrating that the whole amount of Pt disappeared from the graphite in 120 h. There was only a minor change detectable after the first 24 h (fig. 1c). It is important to note, however, that the voltammograms reflect only the number and distribution of surface active sites able to adsorb hydrogen, not the whole amount of platinum. That is, metal dissolution could occur in the first 24 h as well, at nearly constant surface characteristics. The series of voltammograms shown in fig. 1 provide unambiguous evidence for the complete dissolution of supported Pt in 120 h during the oxidation of sorbose under very mild conditions.

Corrosion of Pt supported on graphite paste showed different characteristics. The slow but continuous decrease of surface Pt atoms exposed to hydrogen sorption is illustrated in fig. 2. The amount of adsorbed hydrogen decreased after 120 h sorbose oxidation by a factor of more than 3 (fig. 2b), compared to the original amount measured before sorbose oxidation (fig. 2a).

Leaching of Pt supported on HOPG is shown in fig. 3. After 24 h reaction time a significant growth of the platinum surface area is indicated by the increased area under the hydrogen sorption and ionization peaks of the cyclic voltammogram (fig. 3b). The roughening of the Pt particles continued till 72 h (fig. 3c). After 120 h reaction time, the total amount of Pt was dissolved as indicated by the absence of hydrogen sorption peaks characteristic of Pt (fig. 3d). The voltammograms of HOPG support measured before Pt deposition and after using the Pt/HOPG for 120 h are considerably different. This change is attributed to a modification of the well-defined, atomically flat HOPG surface during L-sorbose oxidation and platinum dissolution. The modification of the HOPG surface can be of structural or chemical nature including rearrangement of graphite, contamination by organic residues or partial oxidation. Note that the voltammogram of HOPG after reaction (fig. 3d) is rather similar to that of the graphite tablet (fig. 1a), and the latter type of commercial graphite possesses a relatively large surface area, O-containing surface functional groups and impurities.

In order to reveal the oxidation state of Pt during sorbose oxidation, the potential of Pt after various pretreatments was monitored as a function of reaction time (fig. 4). Interestingly, after 30 min reaction the electrode potential was around 900 mV, independent of the initial oxidation state of Pt (untreated sample after storing in air, strongly preoxidized or prereduced surfaces). Moreover, this steady-state catalyst potential is very close to the stabilized potential of a 5 wt% Pt/alumina (ca. 800–850 mV) measured during sorbose oxidation in a slurry reactor under strikingly different reaction conditions [16].

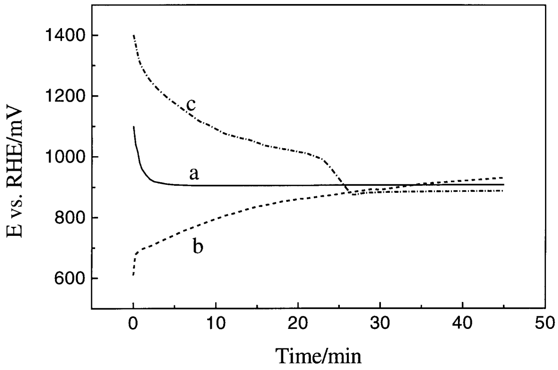

Fig. 4. Time vs. open circuit potential of Pt electrodes immersed into 40 g $\ell^{-1}$ aqueous sorbose solution (pH = 7.2) without stirring; (a) Pt stored in air (slightly oxidized surface), (b) Pt after reductive pretreatment, (c) Pt after oxidative pretreatment (pretreatments: polarization with 100 mA current for 2 min in 0.5 mol $\ell^{-1}$ $H_2SO_4$).

### 3.2. Scanning tunnelling microscopy

The significant increase of the surface of Pt deposited onto HOPG can be explained by the relatively large particle size of Pt in the original (unused) catalyst. Partial leaching of the metal during sorbose oxidation increases the roughness of the particles, resulting in higher amount of adsorbed hydrogen (fig. 3). This view is supported by (ex situ) STM measurements.

The preliminary STM investigations indicated that it was hardly possible to “find” Pt particles on the HOPG surface, when samples were prepared by the technique discussed in table 1 and shown in fig. 3. The electrochemical deposition of a very small amount of Pt (necessary for the above discussed cyclic voltammetric studies) onto low surface area graphite led to the formation of only very few particles, which were difficult to find by approaching the tunnelling tip to the surface. It is likely that not only the extremely low specific surface area of HOPG, but also its hydrophobicity hindered the even distribution of Pt in small particles. A considerable increase of the amount of deposited Pt solved this problem, though the particle size of Pt is expected to further grow with increasing Pt content.

The STM pictures of Pt/HOPG are similar to those reported earlier by Lee et al. [23] and Zubimendi et al. [24]. In other cases, where the preparation technique was different or the HOPG was pretreated before Pt deposition, the reported micrographs [21,22] are rather different from those observed in our laboratory, expectedly.

Leaching of Pt from a Pt/HOPG catalyst during sorbose oxidation is illustrated in fig. 5. The sample was emerged into an aqueous L-sorbose solution in open air, in the liquid cell of the STM. No mixing or air bubbling was applied, similarly to the measurements discussed in the previous chapter. STM images in every 15–20 min were obtained on this Pt/HOPG sample in aqueous L-sorbose solution; two of them are shown in fig. 5. The images were obtained over a period of ca. 2 h from the same surface region by aligning the imaging frame with characteristic landmark features to counteract the instrumental drift.

The images presented in fig. 5 do not indicate a radical transformation of the surface morphology, but some notable changes are observable during the 2 h time period of sorbose oxidation. White colour indicates the top of the Pt particle. The biggest difference in depth here is 11 nm, about 25 atomic layers. Considerable leaching can be seen even in this short period. For example, the group of small crystallites on bottom middle-left, which

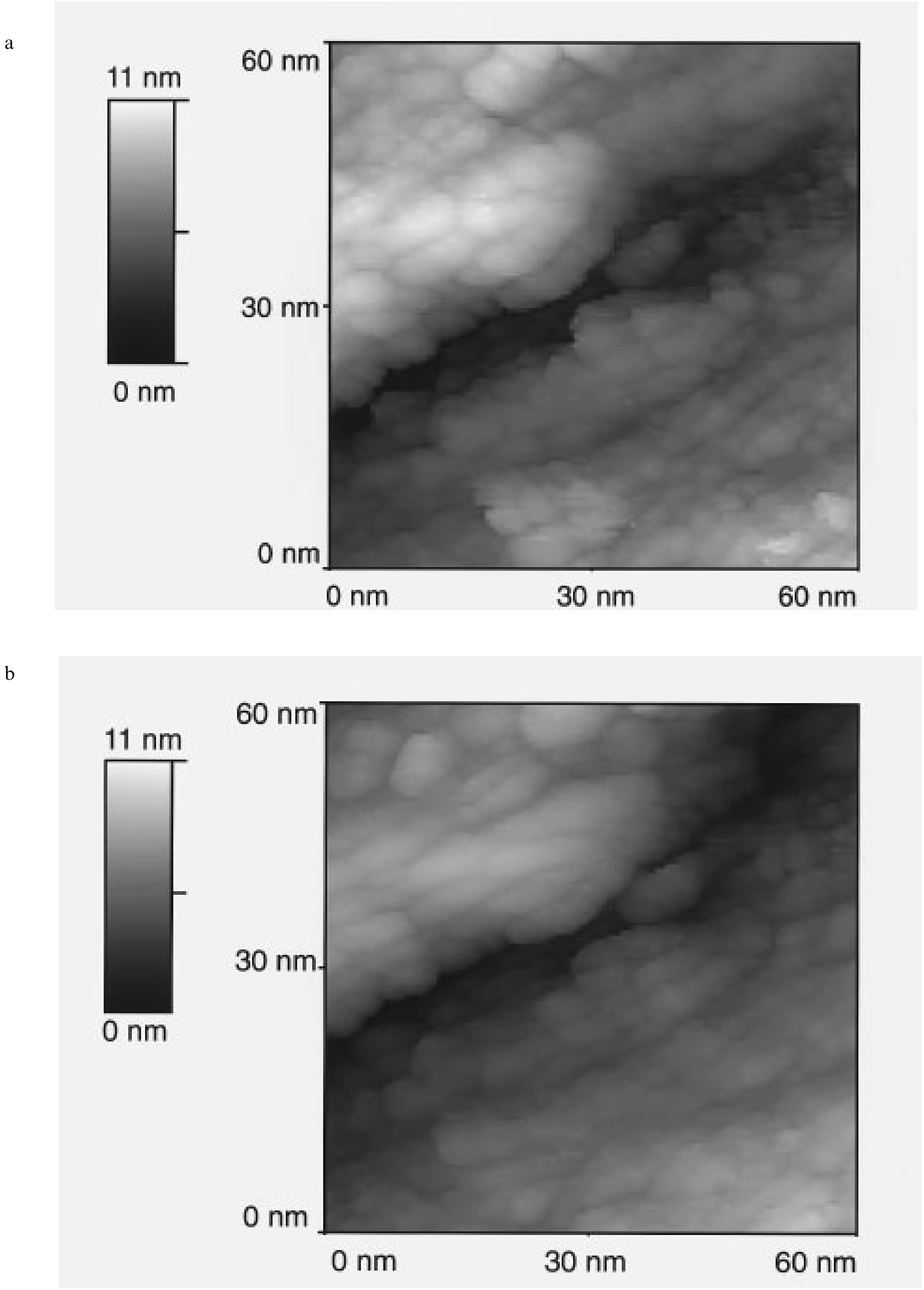

Fig. 5. In situ STM images taken on Pt/HOPG in aqueous L-sorbose solution. Time interval between (a) and (b) 115 min. The micrographs represent 60 × 60 nm areas (tunnelling current: 1 nA, sample bias: 70 mV).

extend above the surroundings in fig. 5a, gradually disappear in the successive images. Corrosion of the white, overlooking kinks in middle left, and the remarkable changes on top right are also clearly noticeable.

The STM pictures obtained with Pt/HOPG in the absence of aqueous sorbose solution were very similar to those shown in fig. 5, which excludes the possibility that the "rolling hill features" result from agglomeration of organic molecules on the surface. Surface roughness statistics indicated a small but significant change during the in situ corrosion studies. During the time period represented in fig. 5 (115 min), the maximum height difference ($Z_{\max} - Z_{\min}$) increased from 11.1 to 12.4 nm in 90 min, then decreased again to 10.7 nm. Similarly, the area RMS (square root of area average of $\Delta Z^2$) increased from 1.94 to 2.01 nm, then decreased to 1.86 nm.

The in situ investigation of Pt corrosion during sorbose oxidation has also been performed with platinum deposited onto a 1 × 1 cm Pt foil. These experiments provided very similar results: clearly detectable uneven corrosion of Pt in a time scale of 0.5–2 h.

## 4. Discussion

The combined voltammetric and in situ STM investigations provided unambiguous evidence of a considerable corrosion of platinum in the course of L-sorbose oxidation with molecular oxygen. Despite the very mild conditions (neutral aqueous solution at room temperature), either the total amount of Pt dissolved from the support (HOPG and high surface area graphite) or at least a significant loss in the number of surface Pt atoms was observed. The morphology of Pt, influenced by the nature of support and the preparation method, affects the rate of Pt leaching, but even in the best case the loss of noble metal is significant.

It was shown that the potential of a Pt electrode catalyst during sorbose oxidation is very similar to that measured in a slurry reactor using a Pt/alumina (powder) catalyst [16]. This is an indication that the relative rates of oxygen transport from the gas phase to the Pt surface (compared to the rate of the surface chemical reaction), and accordingly, the oxidation state of Pt are similar in the two systems. The stabilized potential of Pt/alumina (0.8–0.85 V [16]) and Pt (0.9 V) are in a potential range where metallic platinum is rather stable in neutral aqueous medium [33]. The considerable corrosion of Pt during sorbose oxidation is attributed to the formation of 2-KLG, a polyhydroxy ketoacid with excellent chelating properties. (HPLC analysis of the product composition has been reported earlier [16]). A possible way to avoid or at least minimize the leaching of Pt is to increase the pH of the solution and avoid the presence of free carboxylic acid. However, it was shown [16] that the poor stability of the product 2-KLG at pH higher than 7.5 limits the oxidation reaction to neutral solutions.

## 5. Conclusions

Combined cyclovoltammetric and in situ STM studies performed on various platinum/graphite model catalysts, exposed to conditions typical for the catalytic oxidation of L-sorbose to 2-keto-L-gulonic acid by air, revealed that platinum restructures and dissolves under these conditions. Platinum corrodes as a result of the interaction with the carboxylic acids formed. The partial oxidation of polyhydroxy compounds to the corresponding carbonyl compounds, carboxylic and dicarboxylic acids over Pt metals in aqueous solution is a frequently used process due to the obvious technological and environmental advantages and the lack of other solid catalysts with comparable selectivity. However, our study demonstrates that Pt metals may not be suitable catalysts, when the product is an acid with good chelating properties.

## Acknowledgement

Financial support of this work by the Swiss National Foundation (Support Program "Eastern Europe") is kindly acknowledged. Thank is also due to F. Atamny for fruitful discussions and his technical help in the STM investigation.

## References

[1] J. Fried and J.A. Edwards, *Organic Reactions in Steroid Chemistry*, Vol. 1 (Van Nostrand Reinhold, New York, 1972) p. 329.
[2] A.H. Haines, *Methods for the Oxidation of Organic Compounds* (Academic Press, London, 1988) p. 158.
[3] T. Mallat and A. Baiker, Catal. Today 19 (1994) 247.
[4] K. Heyns and H. Paulsen, Adv. Carbohyd. Chem. 17 (1962) 169.
[5] H. Röper, in: *Carbohydrates as Organic Raw Materials*, ed. F.W. Lichtenthaler (VCH, Weinheim, 1990) p. 267.
[6] H. van Bekkum, in: *Carbohydrates as Organic Raw Materials*, ed. F.W. Lichtenthaler (VCH, Weinheim, 1990) p. 289.
[7] H. Kimura, K. Tsuto, T. Wakisaka, Y. Kazumi and Y. Inaya, Appl. Catal. A 96 (1993) 217.
[8] M. Besson, F. Lahmer, P. Gallezot, P. Fuertes and G. Flèche, J. Catal. 152 (1995) 116.
[9] B.M. Despeyroux, K. Deller and E. Peldszus, Stud. Surf. Sci. Catal. 55 (1990) 159.
[10] P.C.C. Smits, B.F.M. Kuster, K. van der Wiele and H.S. van der Baan, Appl. Catal. 33 (1987) 83.
[11] K. Heyns, Ann. 558 (1947) 177.
[12] M. Hronec, Z. Cvengrosova, J. Tuleja and J. Ilavsky, Stud. Surf. Sci. Catal. 55 (1990) 169.
[13] C. Brönnimann, T. Mallat and A. Baiker, J. Chem. Soc. Chem. Commun. (1995) 1377.
[14] C. Brönnimann, Z. Bodnar, R. Aeschiman, T. Mallat and A. Baiker, J. Catal. 161 (1996) 720.

[15] T.C. Crawford and S.A. Crawford, Adv. Carbohydr. Chem. Biochem. 37 (1980) 79.

[16] C. Brönnimann, Z. Bodnar, P. Hug, T. Mallat and A. Baiker, J. Catal. 150 (1994) 199.

[17] Y. Schuurman, B.F.M. Kuster, K. van der Wiele and G.B. Marin, Appl. Catal. A. 89 (1992) 47.

[18] G. Witek, M. Noeske, G. Mestl, Sh. Shaikhutdinov and R.J. Behm, Catal. Lett. 37 (1996) 35.

[19] M. Komiyama, J. Kobayashi and S. Morita, J. Vac. Sci. Technol. A 8 (1990) 608.

[20] S. Eppell, G.S. Chottiner, D.A. Scherson and G. Pruett, Langmuir 6 (1990) 1316.

[21] X.C. Zhou and E. Gulari, Acta Cryst. A 47 (1991) 17.

[22] K.L. Yeung and E.E. Wolf, J. Catal. 135 (1992) 13.

[23] S. Lee, H. Permana and K.Y.S. Ng, Stud. Surf. Sci. Catal. 75A (1993) 1863.

[24] J.L. Zubimendi, L. Vàzquez, P. Ocòn, J.M. Vara, W.E. Triaca, R.C. Salvarezza and A.J. Arvia, J. Phys. Chem. 97 (1993) 5095.

[25] P. Gallezot, in: *Catalyst Characterisation*, eds. B. Imelik and J.C. Vedrine (Plenum Press, New York, 1994) p. 675.

[26] F. Atamy, D. Duff and A. Baiker, Catal. Lett. 34 (1995) 305.

[27] J.L. Zubimendi, G. Andreasen and W.E. Triaca, Electrochim. Acta 40 (1995) 1305.

[28] Kh.Z. Brainina and M.B. Vydrevich, J. Electroanal. Chem. 121 (1981) 1.

[29] I. Bakos and G. Horányi, J. Electroanal. Chem. 397 (1995) 105.

[30] R. Woods, in: *Electroanalytical Chemistry*, Vol. 9, ed. A.J. Bard (Dekker, New York, 1976) p. 1.

[31] J.M.H. Dirkx and H.S. van der Baan, J. Catal. 67 (1981) 1.

[32] J.M.H. Dirkx, H.S. van der Baan and J.M.A.J.J. van den Broek, Carbohyd. Res. 59 (1977) 63.

[33] M. Pourbaix, *Atlas of Electrochemical Equilibria in Aqueous Solutions* (Nat. Assoc. of Corrosion Eng., Houston, 1974) p. 378.